

## Covalent Bond Connectivity, Medium Range Order, and Physical Properties in TeX and TeXAs Glasses

HONG-LI MA, XIANG-HUA ZHANG, AND JACQUES LUCAS

*Laboratoire de Chimie Minérale, Université de Rennes I Avenue du Général Leclerc, 35042 Rennes Cédex, France*

AND HEMA SENAPATI, ROLAND BOHMER, AND C. AUSTEN ANGELL

*Department of Chemistry, Arizona State University, Tempe, Arizona 85287*

Received July 12, 1991

Data on the new As–Te–Se–I glasses are analyzed to determine whether the extended order determined by bond connectivity via the average coordination number,  $\langle r \rangle$ , controls the physical properties as it does in the case of the Ge–As–Se system. When appropriate allowance is made for partial 4-coordination of Te in Te- and I-rich glasses, the calorimetric glass transition temperature  $T_g$  is found to be a universal function of  $\langle r \rangle$  as in Ge–As–Se (4-3-2) glasses. However, no special behavior is found at the Phillips–Thorpe rigidity percolation threshold value,  $\langle r \rangle = 2.4$  as in the 4-3-2 case. The  $\langle r \rangle$ -dependences of both linear and non-linear aspects of relaxation appear smaller in the present system, and no extrema are in evidence. This is interpreted to indicate that the 2- vs 3-dimensional nature of crosslinking, by As vs. Ge, respectively, of the basic chain structures obtained at all  $\langle r \rangle = 2$  compositions, is an important property-controlling factor. © 1992 Academic Press, Inc.

### Introduction

In the structure of complex crystals one usually recognizes the existence of two types of order, one involving the tightly bonded groups such as  $(\text{SiO}_4)$ ,  $(\text{NO}_3)$ ,  $(\text{TaF}_6)$ ,  $(\text{C}(\text{CH}_3)_4)$ , etc., and a second involving the often subtle arrangements of these species with the neutralizing cations and anions (and sometimes also with neutral solvating species). The latter may be regarded as the “extended order” of the crystal. A third, more subtle, and longer range ordering is that which distinguishes one crystal polytype from others. This subject is being given increasing recognition in solid state chemistry at the moment, particularly under

the influence of their importance in the understanding of high  $T_c$  superconductors. With these developments the conceptual gap between the solid state chemistry of the crystalline state and that of the glassy state begins to seem less and less important.

In glassy solids there exists also an important distinction between short range order and medium range, or extended, order. The short range order, which is usually well-defined, dominates certain characteristics such as electronic conductivity ( $I$ ). On the other hand, there is now reason to believe that many of the rheological, mechanical, and thermodynamic properties of glasses, particularly near the glass transition temperature  $T_g$ , are determined by longer range

bonding topologies which take the place of the extended order of the crystalline state. In the present paper we utilize data acquired in the course of evaluating the materials potential of the covalently bonded glasses formed from the elements Te, Se, and halogens (TeX glasses (2)) and Te, Se, halogen, and As (TeXAs glasses (3)) to illustrate the manner in which the extended order determined by bond connectivity plays a leading role in fixing the physical properties of the glass-forming system.

The TeX and TeXAs systems, which are currently a source of some excitement because of their unique combination of optical properties (transmission to almost 20  $\mu\text{m}$ ) with stability against crystallization and moisture attack, in fact have a number of features in common with the much studied systems Ge-As-Se (4-6) and Ge-As-Se-Te (7). The only difference lies in a downward shift in the valence of the elements at the high and low valence ends: tetravalent Ge is dropped and monovalent halogen is added (i.e., if Ge-As-Se is a 4-3-2 glass, As-Se-I and As-Se-Te-I are 3-2-1 glasses). In common remains the mixing of covalently bonding atoms of variable valence, and the consequent generation of a statistical network, the connectivity of which depends on the proportions of the different elements incorporated. We therefore give an initial section to reviewing some of the findings for the better known 4-3-2 systems, in order to provide a phenomenological framework within which to examine the observations for the new glasses.

The system Ge-As-Se, in which there is a minimum variation in atomic mass and electronegativity for the changes in valence, has been adopted as a model system for covalently bonded glass studies. Since the detailed studies of Webber and Savage (4), the system has been recognized as an ideal testing ground for the ideas of Phillips (8) and Thorpe (9) on optimized covalent bond distributions and "rigidity percolation" (9).

These authors argued that if covalently bonding atoms are allowed to bond randomly subject to constraints of fixed bond angles and bond lengths, then a special situation is found when the average number of bonded neighbors  $\langle r \rangle$  reaches 2.4. When  $\langle r \rangle$ , which is related to the mole fractions of 4-, 3-, and 2-bonding components by the expression

$$\langle r \rangle = 4X_{\text{Ge}} + 3X_{\text{As}} + 2X_{\text{Se}}, \quad (1)$$

reaches 2.4 the number of degrees of freedom exactly balances the number of constraints, giving an optimized strainfree and rigid bonding scheme (8, 9).

While the original prediction (9) that this rigidity percolation threshold would be manifested by an abrupt increase in the various mechanical moduli for any combination of components with  $\langle r \rangle = 2.4$  has not been borne out experimentally (6, 10),<sup>1</sup> it has recently been found (6, 11) that various other properties characterizing the changeover from (ergodic) liquid to (nonergodic) glassy states show extrema near the  $\langle r \rangle = 2.4$  composition line. In particular, it has been found that the deviation from Arrhenius law behavior of the viscosity and the stress relaxation time (the so-called "fragility" (12)), and also the deviations from exponential and linear relaxation behavior, are minimized at  $\langle r \rangle = 2.4$ . These properties have a very important bearing on the materials processing and applications aspects of glasses, so their dependence on glass composition (via the bond connectivity) is important to understand and will be dealt with in some detail in this paper.

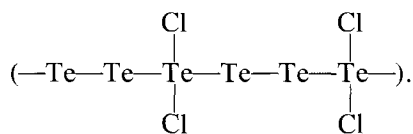
It must be expected that, although the optimized bonding condition can be met in any system which mixes valences on either side of 2.4, some differences will be found

<sup>1</sup> Indeed, it was a subsequent prediction of Thorpe that, in the presence of weaker Van der Waals interactions between unbonded neighbors, the sharp threshold predicted by the simple theory would be smeared.

TABLE I  
GLASS TRANSITION TEMPERATURE FOR  
DIFFERENT COMPOSITIONS

Glass family	Composition	$T_g(^{\circ}\text{C})(\pm 1^{\circ}\text{C})$
$\text{Te}_2\text{Se}_{7-x}\text{IAs}_x$	$\text{Te}_2\text{Se}_7\text{I}$	58
	$\text{Te}_2\text{Se}_6\text{IAs}$	76
	$\text{Te}_2\text{Se}_5\text{IAs}_2$	87
	$\text{Te}_2\text{Se}_4\text{IAs}_3$	111
	$\text{Te}_2\text{Se}_3\text{IAs}_4$	117
	$\text{Te}_2\text{Se}_2\text{IAs}_5$	136
$\text{Te}_{5-x}\text{Se}_3\text{I}_2\text{As}_x$	$\text{Te}_5\text{Se}_3\text{I}_2$	65
	$\text{Te}_4\text{Se}_3\text{I}_2\text{As}$	73
	$\text{Te}_3\text{Se}_3\text{I}_2\text{As}_2$	80
	$\text{Te}_2\text{Se}_3\text{I}_2\text{As}_3$	89
	$\text{TeSe}_3\text{I}_2\text{As}_4$	101
	$\text{Te}_3\text{Se}_6\text{IAs}_x$	$\text{Te}_3\text{Se}_6\text{I}$
$\text{Te}_{0.5}\text{Se}_6\text{IAs}_{2.5}$	$\text{Te}_2\text{Se}_6\text{IAs}$	76
	$\text{TeSe}_6\text{IAs}_2$	82
	$\text{Te}_{0.5}\text{Se}_6\text{IAs}_{2.5}$	95

depending on whether the higher valence is 3 or 4, since the dimensionality of the bonded structure will differ. The 1-dimensional chain structure can be achieved by any combination of valences which gives an average coordination number  $\langle r \rangle$  of 2. For instance, this is achieved by pure Se or by combinations of Te and halogen in which one Te for every two halogens acts in a 4-valent manner, giving the chain structure



This bonding pattern is found in the crystalline compound  $\text{Te}_3\text{Cl}_2$  (13) and assumed (3) to dominate the structure of the vitreous form of this compound and its out. analogues with Br and I. In the  $\text{TeX}$  glasses ( $\text{Te}-\text{Se}-\text{I}-\text{Br}$ ) (which are effectively 4-2-1 glasses with  $\langle r \rangle$  restricted to values near 2), the elements of this chain are assumed to mix at the atomic level with the  $-\text{Se}-\text{Se}-$  elements of pure Se glass to give a sort of

“vitreous solid solution” which retains the 1-dimensional character of its end compositions (3). Introduction of an element like As or Sb will then cause cross-linking of the chains formed by the 2-coordinating Se atoms (or the  $\text{Te}-\text{X}-\text{Se}$  combinations of the  $\text{TeX}$  glasses) to give a locally 2-dimensional topology when multiple cross-links are present. On the other hand, addition of elements like Ge or Sn will introduce 3-dimensional network links. So far there have been no comparisons of behavior of systems like  $\text{Ge}-\text{As}-\text{Se}$  with systems which achieve the Eq. (1) condition in the absence of Ge, except for the binary  $\text{As}-\text{Se}$  system itself, which however, has been found anomalous (6).

We therefore now present some of the findings for  $\text{TeX}$  and  $\text{TeXAs}$  glasses and examine them, and their relation to similar properties in other systems, in the light of the optimized bond distribution ideas outlined above.

## Experimental

Glasses were prepared from high purity elements as described in Ref. (3). All the elements were treated to remove the surface oxide. Te was cleaned by a solution of  $\text{HBr} + \text{Br}_2$ . Se and As were heated under vacuum respectively to 250 and 350°C, and the  $\text{I}_2$  was purified by sublimation. The compositions prepared are available in Table 1.

Glass transition temperatures,  $T_g$ , were determined using a SETARAM DSC 92 and the heating rate was 10°C/min. Other heating rates were used only for examining dependence of  $T_g$  on this experimental condition.

Glasses of different compositions were annealed at different temperatures and for different times in order to determine the dependence of  $T_g$  on both time and temperature of annealing.

The viscosity was obtained using both the

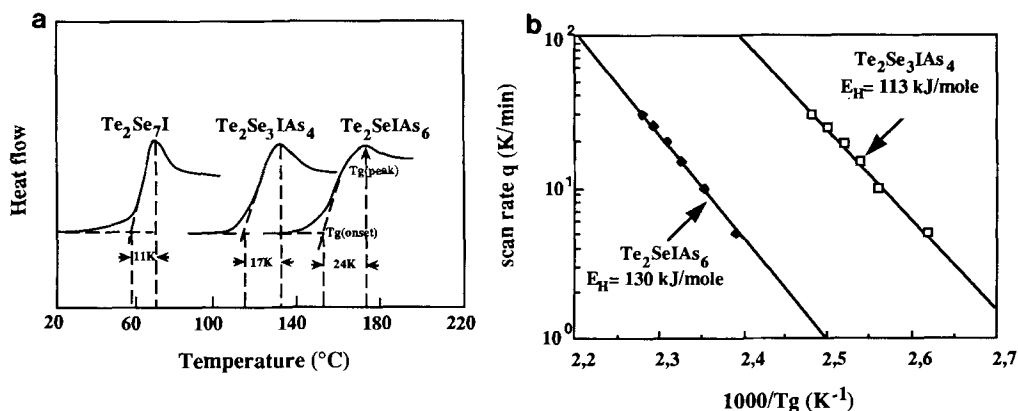


FIG. 1. (a) DSC scans for three phases in the  $\text{Te}_2\text{Se}_{7-x}\text{IAs}_x$  system defining  $T_g$  (onset) and  $T_g$  (peak); note the different  $\Delta T_g$  values. (b) Scan rate dependence of  $T_g$  for two  $\text{TeXAs}$  glasses.  $E$  is the calculated activation energy and is a lower bound on the true enthalpy relaxation activation energy.

beam bending and penetrometry methods in the viscosity range of  $10^9$ – $10^{15}$  poises.

Finally, to obtain direct information on the linear relaxation function, the relaxation of tensile stress generated by imposition of a step strain was measured using the automated Rheovibron technique described recently (11(a)).

## Results

The results of the  $T_g$  determinations are summarized in Table I. The values cited are for the *onset* temperature defined in Fig. 1. These will be the values referred to in the remainder of the text unless specified otherwise. The  $T_g$  (peak) values differ from the  $T_g$  (onset) values by an amount which depends on composition in a manner which is interesting and which is discussed below.

The calorimetric anomaly at  $T_g$  (onset) depends on thermal history and on the scanning rate,  $q$ . The dependence of  $T_g$  (as determined using a constant heating rate of  $10^\circ\text{C}/\text{min}$  up-scans) on thermal history is shown for two cases in Fig. 2. Figure 2 shows that glasses which have been annealed not too far below  $T_g$  show large overshoots. The transitions

commence at onset temperatures which exceed the "normal"  $T_g$  value by amounts which depend on time and temperature of annealing. This phenomenology has been interpreted in an earlier paper (15) for the case of a  $\text{TeX}$  glass ( $\text{Te}_3\text{Se}_5\text{Br}_3$ ). In the Discussion section we will show that it also depends in an interesting manner on composition.

The viscosity  $\eta$  has so far only been determined for the As-free composition.  $\text{Te}_3\text{Se}_4\text{Br}_3$ , though it is hoped to remedy this situation in the near future. The data are shown in an Arrhenius plot of  $\log \eta$  vs.  $T_g/T$  (Fig. 3). The activation energy is 291 kJ/mol.

Finally we show in Fig. 4 the results of isothermal tensile stress relaxation measurements on the same  $\text{TeX}$  glass whose viscosity is displayed in Fig. 3. The thin lines through the points are plots of the stretched exponential function

$$\Phi = \Phi_0 \exp[-(t/\tau)^\beta] \quad (2)$$

## Discussion

### A. Viscosity

Since it is not only interesting but also vital to the understanding of the glass transi-

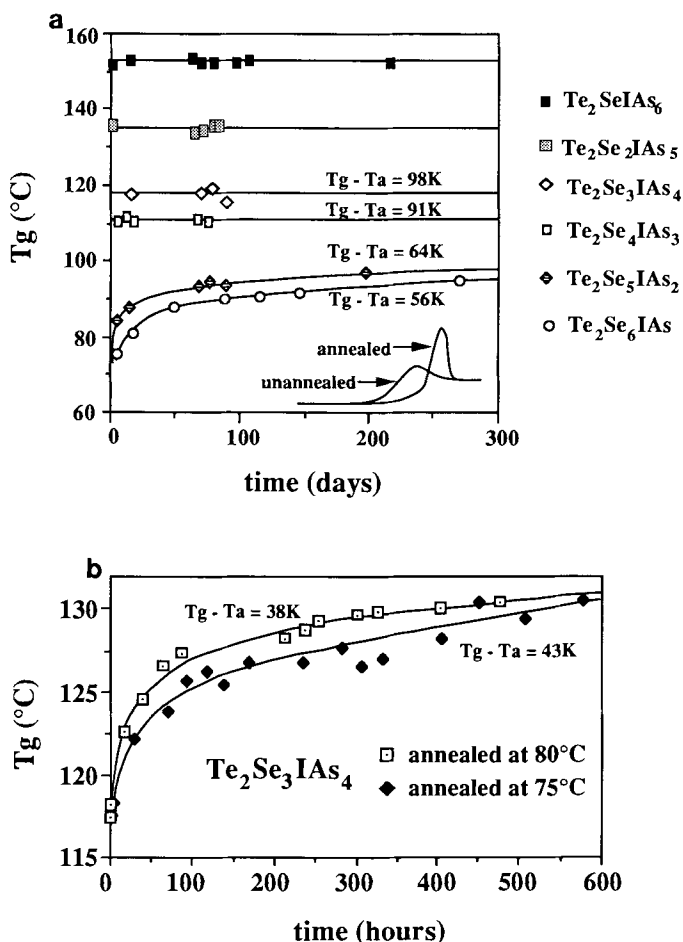


FIG. 2. (a) Dependence of  $T_g$  (onset) on time of annealing at room temperature, 20°C, for glasses in the pseudo-binary system  $\text{Te}_2\text{Se}_7\text{I}-\text{Te}_2\text{IAS}_7$ . The size of the overshoot (seen in the insert) depends on both time and temperature of annealing as discussed in text. (b) Effect of annealing temperature on the value of  $T_g$  (onset) after annealing. Effect of time on the value of  $T_g$  (onset) observed for the glass  $\text{Te}_2\text{Se}_3\text{IAS}_4$ , which showed no effect for room temperature anneals in Fig. 2(a), after annealing at two higher temperatures. Note that the two curves will cross at long enough times.

tion temperature dependence on composition, we first discuss the differences between the viscosity and the relaxation behavior of the  $\text{TeX}$  composition  $\text{Te}_3\text{Se}_4\text{Br}_3$  and pure Se.

These are two liquids in each of which the basic viscosity-determining structure is a chain conformation. However, the chain repeat units are rather different in character.

In Se it is a simple linear chain (albeit plasticized with a variable amount of 8-membered ring molecules (11, 14)), while in the case of the  $\text{TeX}$  glass it is the structure discussed earlier with two side chain halide groups on a statistical number of the tellurium atoms (every 3rd Te in the case of  $\text{Te}_3\text{Cl}_2$ ). In the well-studied case of hydrocarbon chain molecules (16) the presence of the two side

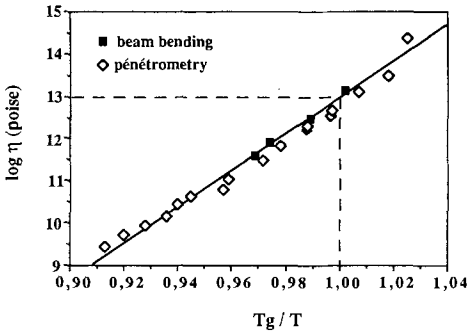
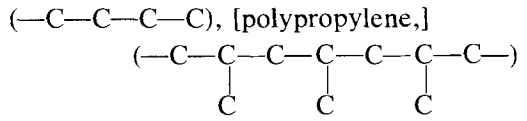
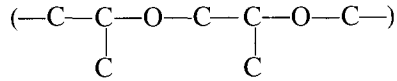


FIG. 3. Viscosity of a TeX glass as function of inverse temperature near  $T_g$ .



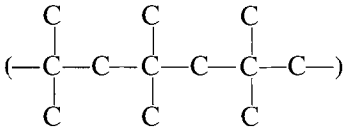
and the more fully amorphous polypropylene oxide (PPO)



are much more fragile (17). To support the structural assignments suggested above, we compare the hydrocarbon and chalcogenide findings in Fig. 5, using chain segment relaxation time data (17) to avoid the large chain length problem in the case of the hydrocarbons. The TeX glass is less fragile than Se, just as PIB is less fragile than PPO.

The correspondences in Fig. 5 suggest that in dealing with TeX and TeXAs glasses rich in Te and halogen some allowance for the 4-coordination of a fraction of the Te atoms will have to be made in assessing the average coordination number. In the presence of sufficient arsenic, however, the halogen will be bound preferentially by arsenic, and Te will return to 2-coordination.

groups on alternating carbons (polyisobutylene) makes a major difference to the fragility (for reasons that are not entirely elucidated). Polyisobutylene (PIB), with the structure



is the "strongest" chain polymer in the Fig. 5 sense, whereas polyethylene,

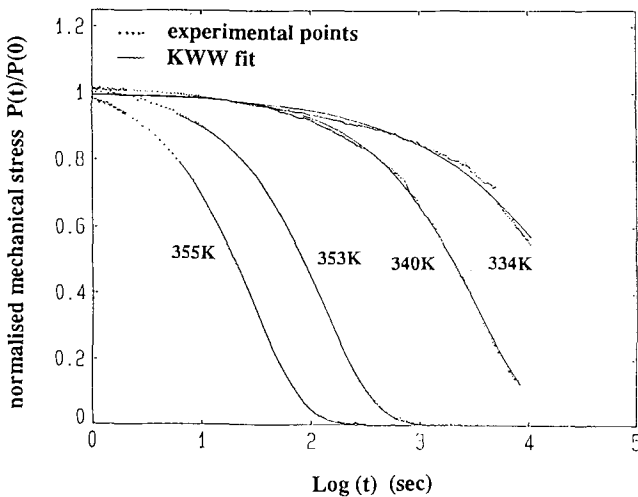


FIG. 4. Decay of mechanical stress due to step strain on a sample of TeX glass as function of time at several temperatures near  $T_g$ .

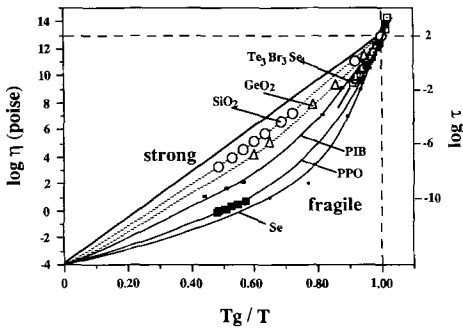


FIG. 5. Comparison of viscosities of inorganic chain polymers. Se (sample) and TeSeBr (with side groups) with hydrocarbon chain polymers polyisobutylene and polypropylene oxide and the strong liquids SiO<sub>2</sub> and GeO<sub>2</sub>, using T<sub>g</sub>-reduced Arrhenius plot.

**B. Heat Capacity**

With these considerations in mind we now turn attention to the interesting matter of the effects of As cross-linking of TeX glasses. First we check to see if, as in the case of the Ge-As-Se system (6), all the T<sub>g</sub> values can be collapsed onto a single line by plotting the data as a function of ⟨r⟩. Here the average coordination number is defined by

$$\langle r \rangle = 3X_{As} + 2X_{Se} + 2X_{Te} + X_I. \quad (3)$$

The results are shown in Fig. 6(a). It is

seen immediately that while the data for Te- and I-poor glasses are well correlated by this procedure, those with high Te and I contents fan out to low ⟨r⟩ values. However, the presence of large Te and I contents establishes exactly the conditions in which a Te coordination number of 4 is to be expected for a part of the Te (one tetravalent Te for each 2I) according to the above discussion. If we correct the ⟨r⟩ values accordingly, we now find (Fig. 6(b)) that the T<sub>g</sub> values for the low ⟨r⟩ glasses fan out in a direction opposite to that in Fig. 6(a), suggesting that the ⟨r⟩ values may have been overcorrected slightly. The slope in Fig. 6 is slightly less than for the Ge-As-Se case in the same ⟨r⟩ range (11), but a common physical origin for the effect is indicated.

The Fig. 6(b) finding immediately raises the question of whether or not the other correlations with ⟨r⟩ found for the Ge-As-Se glasses (6, 11) will also be found in the present system, viz.,

- (i) minima at ⟨r⟩ = 2.4 in the heat capacity jump at T<sub>g</sub>, ΔC<sub>p</sub>, and in the activation energies for viscosity and for mechanical relaxation E<sub>A</sub> and enthalpy E<sub>H</sub> (6), and
- (ii) weak minima or plateau values in the fragility *m* and in the deviations from exponentiality and state dependence of the relax-

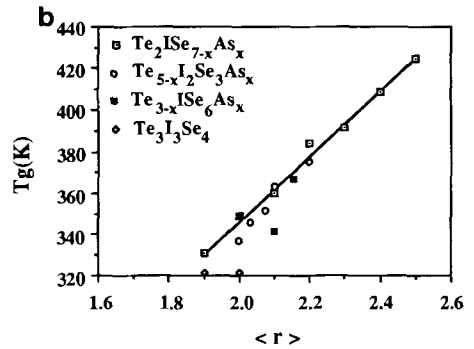
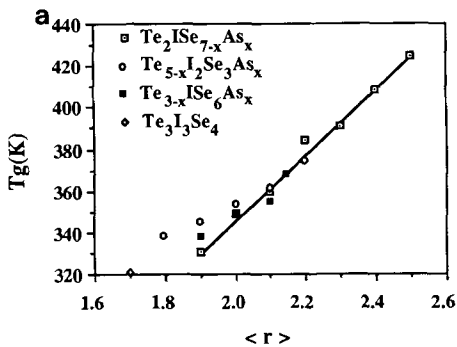


FIG. 6. (a) Variation of T<sub>g</sub> with average coordination number ⟨r⟩ defined by Eq. (3), (b) Variation of T<sub>g</sub> with ⟨r⟩ after allowance for some Te in 4-coordination in Te,I-rich glasses.

ation process (11) near  $\langle r \rangle = 2.4$ . To most of these questions we can give tentative answers on the basis of data now available, as follows.

Considering first the heat capacity jumps, we have observed qualitatively a decrease in the "size" of the glass transition with increasing As content as seen by DSC of approximately equal-sized samples, but since the exact sample masses are not available we cannot at this time give a quantitative verdict. However, the *breadth* of the glass transition, viz.,  $\Delta T_g = (T_g(\text{peak}) - T_g(\text{onset}))$ , does not depend on the sample size, and this was observed, in Ref. (6), to pass through a maximum where the  $\Delta C_p$  at  $T_g$  passes through a minimum. We therefore examine, in Fig. 7(a), the breadth of the glass transition for the present system as a function of  $\langle r \rangle$ , and make a comparison with the data for the system Ge-As-Se using the dimensionless reduced form  $(\Delta T_g)/T_g$ , in Fig. 7(b).

Interestingly enough, although the trend to large breadth with increasing  $\langle r \rangle$  that was seen in Ge-As-Se is reproduced in the present system, the maximum at  $\langle r \rangle = 2.4$  is not. Furthermore, the breadth of the transition (like its appearance as a distinct "jump" in

the DSC scan) at  $\langle r \rangle = 2.4$  is quite different from that of the very smeared-out transition seen at  $\langle r \rangle = 2.4$  in the Ge-As-Se system. This raises the possibility that the extrema observed in the latter system at this coordination may be more strongly linked to the *dimensionality* of the bonding topology than to the connectivity or average coordination number *per se*. Clearly a quantitative study of the heat capacity jump at  $T_g$  will be needed to resolve this question. We would emphasize that this question is very important for the understanding of physical property/extended order relationships in covalent glassy systems.

### C. Stress Relaxation and Structural Relaxation

Finally we consider the available information on the non-exponential and non-linear aspects of the relaxation process, which are the aspects involved in the stress relaxation process illustrated in Fig. 4 and in the process by which the value of  $T_g$  is able to change with time and temperature of annealing as seen in Fig. 2.

For the former we only have data on the TeX glass which, however, can be usefully compared with that for Se and lightly cross-

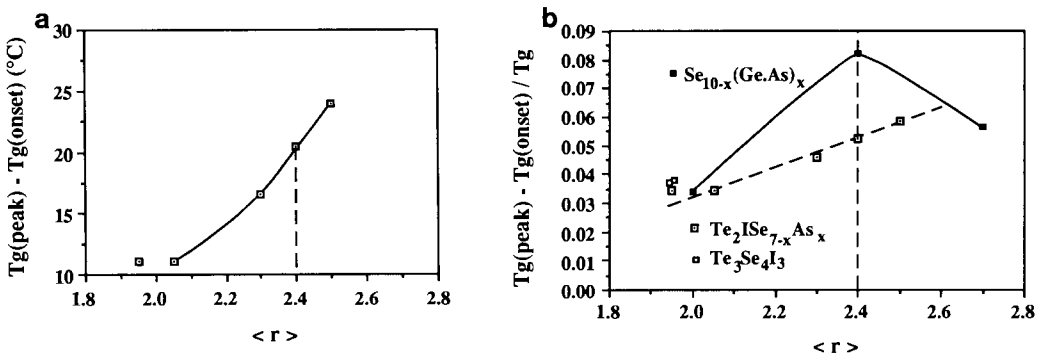


FIG. 7. (a) Breadth of the glass transition in  $\text{Te}_2\text{ISe}_{7-x}\text{As}_x$  glasses. (b) Comparison of reduced breadth of glass transition in TeX and TeXAs glasses vs.  $\langle r \rangle$  with reduced breadth in the 4-3-2 system Ge-As-Se (Ref. (6)). Note the contrast in behavior near  $\langle r \rangle = 2.4$  of the two systems.

linked Se. The TeX glass relaxations show no sign of the separate and dominant shorter time process seen in pure Se glass (11) and attributed to the fraction of Se in 8-membered ring form. Thus, it would seem improbable that there are any ring-like components present in the TeX glass, although they are known to exist in the compounds  $\text{TeCl}_2\text{S}$  and  $\text{TeBr}_2\text{S}$  (18).

The fit of the observed relaxation data to the KWW equation (Eq. (2)) is very good, essentially within the noise in the data. In this case it is interesting that at the glass transition temperature where the relaxation time is 500 sec, the relaxation process is closer to exponential than for glassy Se. This is as would be expected in view of its smaller fragility (see Fig. 5). However, the relaxation is also more exponential than for any of the previous chalcogenide glasses, which is not expected. Before any significance can be attached to this result it must be demonstrated that sample size effects, which have distorted some earlier measurements (11), are not present.

Turning to the non-linear or structural state-dependent relaxation effects, we encounter some of the most challenging phenomenology of this work. The increases observed in  $T_g$  in the annealed glasses of this study (Fig. 2(a) and (b)) are a direct consequence of the fact that the relaxation time for an amorphous structure depends not only on the temperature but also on the structural state of the glass. The analog in the solid state chemistry of crystals is the well-known effect of annealing on the conductivity of ionic substances at temperatures below that at which the defect population became frozen during cooling. Because the ionic conductivity (hence also the electrical stress relaxation time) depends on the number of lattice vacancies present, annealing, which allows the number of defects to decrease toward the equilibrium population, leads to a decrease in the conductivity. Obviously, if the conductivity were decoupled

from the lattice defect population, annealing would have no effect (as in the case of electronic conductivity). The connection of the longer relaxation time to the observation of a higher  $T_g$  on reheating is simply made (as described previously (15)) by noting that the glass transition for a fixed scan rate occurs when the relaxation time decreases to some fixed value (usually ca. 200 sec). If the relaxation time has been increased by annealing then clearly the glass must be heated to a higher temperature before the transition can be observed.

The nature of the "defects" which anneal out in the case of glasses is not so obvious as in the crystal, but they can be conceptualized as loosely packed regions in the amorphous structure which can be eliminated by slow and highly cooperative rearrangements of the surrounding atoms. In polymer glass chemistry it is common (though not wholly accurate) to associate them with "free volume" in the structure. However, it is not necessary to understand their nature in detail in order to understand the annealing effect on  $T_g$ . For the present purposes it is more important to understand that the population of such defects at any temperature determines the disorder in the glass and is closely linked to the excess entropy of the glassy state, which approaches zero at the Kauzmann temperature. The Kauzmann temperature,  $T_K$ , falls very close to  $T_g$  at the fragile liquid limit and approaches to zero K (hence  $T_g/T_K \rightarrow \text{infinity}$ ) in the strong liquid limit. Quantitatively, one finds  $T_g/T_K = (1-16/m)^{-1}$  where  $m$  is the fragility defined by  $m = E_H/(2.303 RT_g)$ , (11, 14).

Since the "strong" limit is approached at  $\langle r \rangle = 2.4$  in Ge-As-Se glasses, the non-linear effects should disappear at this composition and indeed have been observed to do so in mechanical stress relaxation measurements on this system (11). In the present system the ability of  $T_g$  to be increased by the annealing effect is of much practical importance (4), so the possibility of its dis-

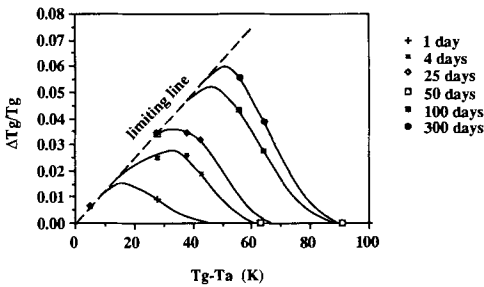


FIG. 8. Dependence of the increase in  $T_g$ , normalized to  $T_g$  after annealing, with the difference between  $T_g$  (unannealed) and the temperature of annealing  $T_a$ , for different annealing times. The limiting line, which is reached for all annealing times when  $T_g - T_a$  is small, shows that  $T_g$  increased for glasses annealed long enough to reach the metastable equilibrium state. Data on several TeX and TeXAs glasses have been used to obtain this diagram. More detailed studies may show some differences in the limiting slope for glasses of different  $\langle r \rangle$  values.

appearing, and the limits on this effect, are necessarily of interest.

The fact that the  $\text{Te}_2\text{Se}_3\text{IAS}_4$  glass, for which  $\langle r \rangle = 2.3$ , still shows a strong annealing effect on  $T_g$  (see Fig. 2(b)) is therefore consistent with the small  $\Delta T_g$  relative to that in Ge-As-Se system at the same  $\langle r \rangle$  (Fig. 7(b)) and the conclusion that there are important differences between the 4-3-2 and 3-2-1 systems with respect to  $\langle r \rangle$ -dependent properties. In fact the Ge-As-Se glass with the same  $\Delta T_g$  as the  $\text{Te}_2\text{Se}_3\text{IAS}_4$  glass has  $\langle r \rangle = 2.1$  and shows large non-linear effects (11).

If we therefore make the simplifying assumption that all the glasses of this study show similar annealing effects, then it is possible to use the results of Fig. 2(a) and (b), Ref. (15), and subsidiary results in Ref. (3) to obtain a diagram which combines the effects of both time and annealing temperature relative to  $T_g$  in a useful and predictive manner. In Fig. 8, the difference between  $T_g$  of the annealed glass,  $T_{g,\text{ann}}$ , and that of the as formed glass,  $T_{g,\text{in}}$ , divided by  $T_g$  is plotted vs. the difference between  $T_g$  and the an-

nealing temperature. Figure 8 shows in at least approximate form the maximum increase in  $T_g$  which could be obtained on waiting sufficient time to reach the equilibrium state (equilibrium "defect" population). It shows what the  $T_g$  value will be if insufficient time is allowed. More detailed studies on selected glass compositions may reveal a small  $\langle r \rangle$  dependence of the slope of the limiting line, but the general form will not be changed.

### Concluding Remarks

While the analysis of TeXAs glass behavior we have given here strongly suggests that the behavior of covalently bonded glasses is not universal with average coordination number amongst all systems, as might have been hoped from initial studies, it remains true that the average coordination number is a powerful variable for reducing behavior within a given system to quasi-universal form. This observation implies the existence of intermediate range orders of different forms, depending on dimensionality of bonding topologies. It will be interesting to follow this line of thought not only through more extensive studies of TeXAs-type glasses, but also through study of other bonding combinations such as 4-2-1, 4-3-1, and 4-3-2-1.

### Acknowledgments

The authors express appreciation for the financial support of this work from the D.R.E.T. (French Ministry of Defense) and from the U.S. Office of Naval Research under Agreement N00014-84-K-0289. We thank C. T. Moynihan for helpful discussions.

### References

- (a) B. A. KHAN AND D. ADLER, *J. Non-Cryst. Solids* **64**, 35 (1984). (b) T. MINAMI, M. HATTORI, F. NAKAMACHI, AND M. TANAKA, *J. Non-Cryst. Solids* **3**, 327 (1970).
- J. LUCAS AND X. H. ZHANG, *J. Non-Cryst. Solids* **104**, 38 (1988).

3. H. L. MA, X. H. ZHANG, AND J. LUCAS, *J. Non-Cryst. Solids*, in press.
4. P. J. WEBBER AND J. A. SAVAGE, *Non-Cryst. Solids* **20**, 271 (1976).
5. C. LE SERGENT, *SPIE* **799**, 18 (1987).
6. H. TATSUMISAGO, B. L. HALFPAP, J. L. GREEN, S. M. LINDSAY, AND C. A. ANGELL, *Phys. Rev. Lett.* **64**, 1549 (1990).
7. J. NISHII, T. YAMASHITA, AND T. YAMAGISHI, *Appl. Opt.* **28**, 5122 (1989).
8. J. C. PHILLIPS, *J. Non-Cryst. Solids* **34**, 153 (1979).
9. M. F. THORPE, *J. Non-Cryst. Solids* **57**, 355 (1983).
10. S. S. YUN, HUI LI, R. L. CAPPELLETTI, R. N. ENZWEILER, AND P. BOOLCHAND, *Phys. Rev. B* **39**, 8702 (1989).
11. (a) R. BOHMER, H. SENAPATI, AND C. A. ANGELL, *J. Non-Cryst. Solids* **133**, (1991). (b) R. BOHMER AND C. A. ANGELL, submitted for publication.
12. C. A. ANGELL, *J. Non-Cryst. Solids* **73**, 1 (1985); **13**, 133 (1991).
13. R. KNIIEPP, D. MOOTZ, AND A. RABENAU, *Anorg. Chem. (Int. Ed.)* **12**, 499 (1973).
14. R. BOHMER AND C. A. ANGELL, submitted for publication.
15. H. L. MA, X. H. ZHANG, J. LUCAS, AND C. T. MOYNIHAN, *J. Non-Cryst. Solids*, in press.
16. J. D. FERRY, "Viscoelasticity of Hydrocarbon Polymers," Wiley, NY (1973).
17. C. A. ANGELL, L. MONNERIE, AND L. M. TORELL, *Symp. Mat. Res. Soc.* **215**, 3 (1991).
18. J. WEISS AND M. PUPP, *Acta Crystallogr., Sect. B* **B28**, 3653 (1972).